



A comparison for a multiscale study of structural lineaments in southern Brazil: LANDSAT-7 ETM⁺ and shaded relief images from SRTM3-DEM

PATRICIA D. JACQUES^{1,2}, ROMULO MACHADO^{2,3*} and ALEXIS R. NUMMER^{2,4}

¹CPRM, Serviço Geológico do Brasil - DIGEOP, Av. Pasteur, 404, Urca, 22290-240 Rio de Janeiro, RJ, Brasil

²Programa de Pós-Graduação em Recursos Minerais e Hidrogeologia, Instituto de Geociências,
Universidade de São Paulo, Rua do Lago, 562, 05508-080 São Paulo, SP, Brasil

³Departamento de Geologia Sedimentar e Ambiental, Instituto de Geociências,
Universidade de São Paulo, Rua do Lago, 562, 05508-080 São Paulo, SP, Brasil

⁴Departamento de Geociências, Instituto de Agronomia,
Universidade Federal Rural do Rio de Janeiro, BR 465, Km 7, 23890-000 Seropédica, RJ, Brasil

Manuscript received on June 16, 2011; accepted for publication on May 31, 2012

ABSTRACT

This paper presents a comparison of descriptive statistics obtained for brittle structural lineaments extracted manually from LANDSAT images and shaded relief images from SRTM 3 DEM at 1:100,000 and 1:500,000 scales. The selected area is located in the southern of Brazil and comprises Precambrian rocks and stratigraphic units of the Paraná Basin. The application of this methodology shows that the visual interpretation depends on the kind of remote sensing image. The resulting descriptive statistics obtained for lineaments extracted from the images do not follow the same pattern according to the scale adopted. The main direction obtained for Proterozoic rocks using both image types at a 1:500,000 scale are close to NS±10, whereas at a 1:100,000 scale N45E was obtained for shaded relief images from SRTM 3 DEM and N10W for LANDSAT images. The Paleozoic sediments yielded the best results for the different images and scales (N50W). On the other hand, the Mesozoic igneous rocks showed greatest differences, the shaded relief images from SRTM 3 DEM images highlighting NE structures and the LANDSAT images highlighting NW structures. The accumulated frequency demonstrated high similarity between products for each image type no matter the scale, indicating that they can be used in multiscale studies. Conversely, major differences were found when comparing data obtained using shaded relief images from SRTM 3 DEM and Landsat images at a 1:100,000 scale.

Key words: Landsat images, remote sensing, SRTM, Santa Catarina, statistics, structural lineaments.

INTRODUCTION

The main objective of this paper is the comparative study of two kinds of products from remote sensing images at two different scales for the identification of structural lineaments.

One type of remote sensing image is obtained using optical systems (LANDSAT 7 ETM⁺), which enhances the physical-chemical characteristics of the targets. The other results from the shaded relief images derived from the Digital Elevation Model (DEM) of an interferometric radar mission (SRTM 3), that is related to the dielectric and geometric properties of the targets.

Correspondence to: Patricia Durringer Jacques

E-mail: patricia.jacques@cprm.gov.br

*Bolsista do CNPq

Although there are limitations imposed by the spatial resolution of the images for the study area (15 meters for LANDSAT and 90 meters for the DEM from SRTM 3) and by the use of only two types of sensor (LANDSAT and synthetic aperture radar), these images allow the generation of a varied range of data that, when used separately or combined, produce excellent information concerning the superficial brittle structures.

In this paper the definition by O'Leary et al. (1976) for lineament is applied, which is "a mappable, simple or composite linear feature of a surface whose parts are aligned in a rectilinear or slightly curvilinear relationship and which differs distinctly from the patterns of adjacent features and presumably reflects a subsurface phenomenon".

Ramli et al. (2010) compared lineaments obtained by two methods: the manual one, based on visual interpretation, and the automatic extraction, based on computer algorithms. They concluded that the user should be aware of the advantages and disadvantages of both methods.

According to Strieder and Amaro (1997), lineaments can be classified into two types. Type-1 lineaments are associated with penetrative structures, such as foliation, schistosity and bedding, and are related to ductile structures. Type-2 lineaments are generally related to brittle structures, expressed by drainage and valley systems.

Lineaments can be positive (*e.g.* ridge trends) or negative (*e.g.* river valleys). For this study, only negative lineaments were manually digitized because they are easier to identify and stressed out by drainage patterns.

The use of remote sensing images promoted advanced knowledge in data processing methodologies applied in the geosciences. Specifically when modeled in Geographic Information System (GIS), improving speed and precision in its execution (*e.g.* Jordan et al. 2005, Guth 2006, Valeriano et al. 2006, Rosseti and Valeriano 2007, Silva et al. 2007, Grohmann et al. 2007).

The extraction of structural lineaments from images derived from SRTM – DEM and LANDSAT has been used separately or together through several methodologies. Masoud and Koike (2006) applied both products for hydrogeological studies, using an automatic acquisition method based on the segment tracing algorithm (Koike et al. 1995). Products derived from SRTM-DEM were applied to identify a large ancient drainage system in Central Amazônia, not identified before in optical or in synthetic aperture radar images (Almeida-Filho and Miranda 2007). Demirkesen (2009) quantified geological structures obtained by on-screen digitizing from SRTM-DEM images derived as: slope, aspect, shaded relief, curvature, DEM segmentation, contours and directional derivatives.

The selected area for this study encompasses three geological domains: the Paleo-Neoproterozoic Catarinense Shield, the Paraná Basin Paleozoic sedimentary rocks and the Mesozoic Serra Geral Formation, which is constituted predominantly of basalts.

For each one of these geological domains, negative lineaments were manually extracted from LANDSAT and shaded relief images from DEM SRTM 3 at 1:500,000 and 1:100,000 scales. The data obtained were compared for each geological domain in order to evaluate the reproducibility of the data independent of scale adopted and to examine the possibility of reactivation of some of these lineaments.

This research tries to answer the following questions:

What are the general directions obtained by each image type at both scales?

Do they belong to the same population?

Can the two types of images be used in multiscale analysis of Type- 2 lineaments?

What are the preferential directions per rock type and sensor?

GEOLOGICAL SETTING

According to Horn Filho and Diehl (1994, 2001) and Horn Filho (2003), the Santa Catarina state, in Southern Brazil, can be divided in five geologic domains (from east to west): the Coastal Province with Quaternary sediments, the Catarinense Shield (Archean, Proterozoic and Cambrian rocks up to 550 Ma.), sedimentary rocks of the Paraná Basin (between 500 and 180 Ma.), the Serra Geral Formation, which is constituted predominantly of basalts (± 130 Ma.), and the Anitápolis and Lages alkaline complexes ($\pm 65-70$ Ma.), besides Cenozoic sediments.

The study area is situated in the southern-central portion of the Santa Catarina state (Fig. 1). The five geological domains are in the study area, thus allowing the analysis of the linear brittle structures and their preferred directions by domain.

The Catarinense Shield consists of granulitic, metavolcanic and metasedimentary rocks and granites. Two major shear zones crosscut the shield, characterized by ductile to ductile-brittle, NE-trending strike-slip faults (Passarelli 1996, Bitencourt et al. 2008).

Another domain, represented by the Phanerozoic sedimentary rocks of the Paraná Basin, consists of the Gondwana sequence in the central part and the Serra Geral Formation in the western part of the study area. The Paraná Basin is characterized by three successive cycles of subsidence, sedimentation and magmatism that occurred from the Ordovician to the Cretaceous, which were interrupted by the movements related to the "Wealdenian Reactivation" and the opening of the South Atlantic (Almeida 1969).

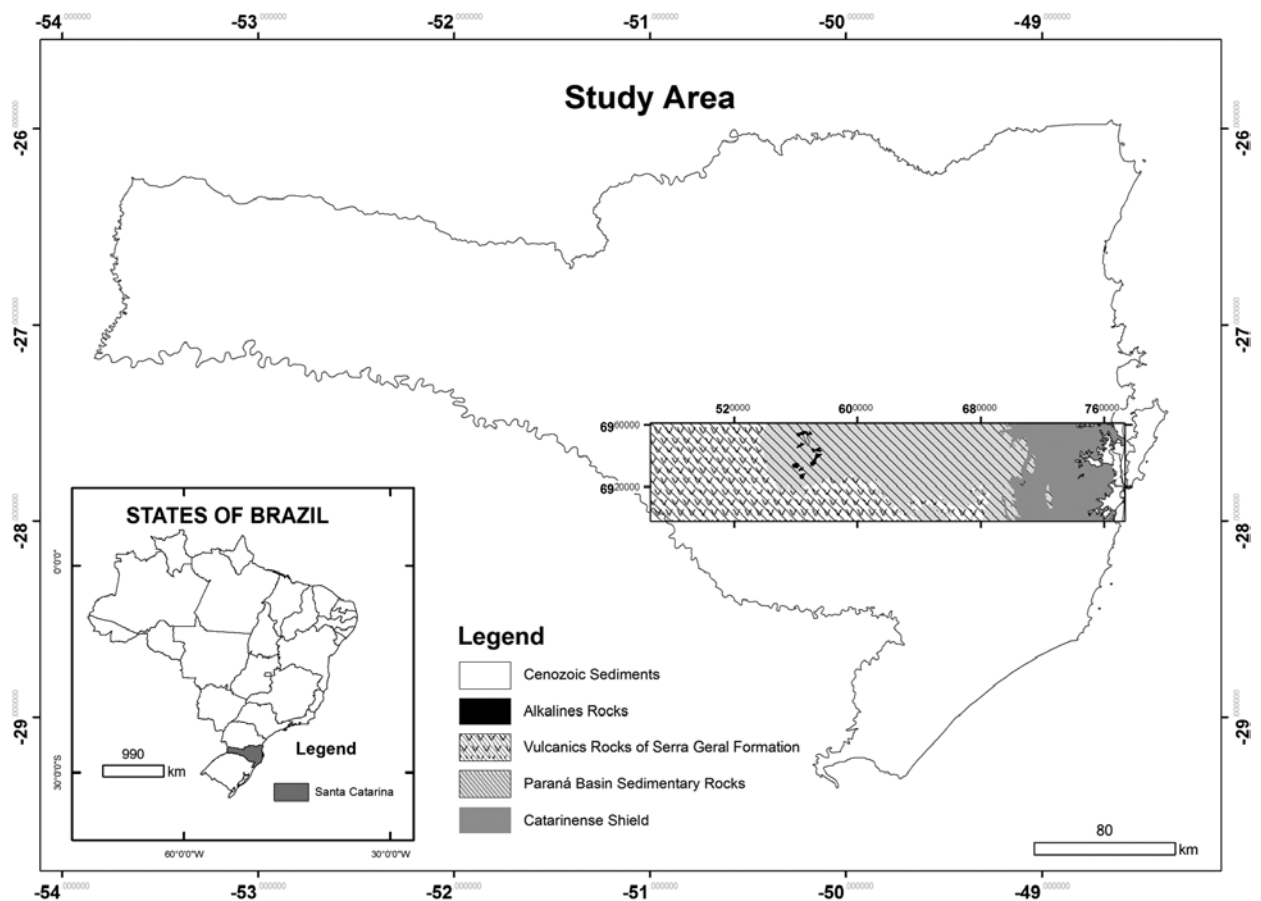


Figure 1 - Study area located in the Santa Catarina State, Brazil. Paraná Basin.

This reactivation was studied by several authors (Almeida 1967, 1986, Piccirillo et al. 1990, Renne et al. 1992) and was responsible for reactivating many structures in the basins and creating new ones. This opening was caused by partial melting of the Tristão da Cunha Plume, which in the Mesozoic would be under the South American Platform (Morgan 1981, O'Connor and Duncan 1990). The effects of lithospheric stretching and the rise of the plume caused distensional igneous activity, generating a significant volume of tholeiitic basalts. The Wealdenian Reactivation started on Neo-Jurassic ending on Eo-Cretaceous and was responsible for the last subsidence of the Paraná Basin allowing the sedimentation of the Bauru Basin, over the Paraná Basin (Almeida 1967).

There are three preferential structural directions in the Paraná Basin: N45-65W, N50-70E and E-W (Zalán et al. 1987, 1991). The first two are older and related to reactivations of its basement. The youngest E-W developed in the Gondwana breakup.

The Lages Dome was the last tectonic structure in the area and is located in the Phanerozoic sedimentary domain, near the volcanic rocks of the Serra Geral Formation. It was an Eo-Cretaceous structure modeled by Roldan (2007) to explain the emplacement of the dome. Two lineament directions (NW and NE) stand out. The NW structures were reactivated in the Eo-Cretaceous and penetrated by dykes. The NE structures are associated with strike-slip faults that affected the alkaline rocks of the Lages Dome (Table I).

MATERIALS AND METHODS

Two types of images were used in this study, one obtained by the LANDSAT ETM⁺ 7 satellite (Level 1G Product Generation System) and the other by the SRTM (Shuttle Radar Topography Mission) (Farr et al. 2007). All images were freely acquired from the USGS (United States Geological Survey) - <http://glovis.usgs.gov> and <http://seamless.usgs.gov> and from the GLCF (Global Land Cover Facility) - <http://glcf.umd.edu/data>.

The LANDSAT images used are identified as 220_079 (03/10/2002) and 221_079 (11/12/2002). Atmospheric correction was applied to bands 1, 2, 3, 4, 5 and 7 to reduce the influence of the molecules of atmospheric gases. The effects of such interference will vary depending on the wavelength of the incident radiation (Turner et al. 1971). The method applied is the "Simple Dark Pixel Subtraction" (Chavez Jr 1975) which consist in the identification of dark values areas, as shadows or water, and the subtraction of this value for each band. The value for each band used in this study is present in Table II. The scenes were merged in one mosaic through a color balancing, fixing the scene 221_079 (largest size of the study area) and adjusting the scene 220_079 (smaller size of the study area). To perform the fusion of the bands 1, 2, 3, 4, 5 and 7 with the panchromatic band (band 8), to achieve a spatial resolution of 15 meters in all bands, the bilinear algorithm was applied in the HSV (Hue, Saturation, Value) method (Carper et al. 1990). A high-pass filter at a 3x3 window was used before lineament extraction.

The SRTM DEM data are provided in three spatial resolutions: (a) 30 arc second (1 km) SRTM-GTOPO 30 of the world; (b) 3 arc second (90 m) of the world; and (c) 1 arc second (30 m) of the USA. For this study the resolution of the data is 3 arc second (90 m), that was resampled by cubic convolution to 30 m, in order to improve the shaded relief derived images with significant gains for visual interpretation and lineaments extractions. Shadow relief images were produced for the following azimuths: 0°, 45°, 90° and 315°. The inclination used for all the shaded relief was 45° based in the Crepani and Medeiros (1994) publication, which suggests this value for shaded relief interpretations.

Although the planimetric accuracy of the SRTM 3 - DEM is nearly 20 meters (Rodrigues et al. 2011) and the planimetric accuracy of LANDSAT 7 ETM⁺ images ranges from 30-50 meters (<http://landsat.usgs>).

gov/geometric_accuracy.php), no additional geometrical corrections were done, as the data were cluster in groups of main directions for comparison.

The linear brittle structures were manually extracted according to the visual interpretation of 1:500,000 and 1:100,000 scales fixed image, totaling four products (Fig. 2): (a) LANDSAT at 1:100,000 scale; (b) SRTM at 1:100,000 scale; (c) LANDSAT at 1:500,000 scale and (d) SRTM at 1:500,000 scale.

Each product was interpreted separately according to the geological domain and age, namely: Proterozoic, Paleozoic and Mesozoic (Fig. 2).

The descriptive statistics (mean, mode and circular variance) were calculated according to Mardia (1972), for the comparison of the data, as shown below.

Each group was organized as bidirectional data in 30° intervals and from 0° to 180° (Table III).

The mean is based on the resultant vector, which has as components the mean direction angle (X_0) and the length of the mean vector (R), based on the Pythagoras Theorem.

Equation 1 was used to calculate the mean direction angle (X_0), and Equation 2 to calculate

the length of mean vector (R). The R value reflects the dispersion, so that a high R value indicates low variability.

$$X_0 = \arctan (S/C) \quad (\text{Eq. 1})$$

$$R = (C^2+S^2)^{1/2} \quad (\text{Eq. 2})$$

where: $C = \frac{1}{n} \sum_{i=1}^n \cos \phi_i$ $S = \frac{1}{n} \sum_{i=1}^n \sin \phi_i$

(C = Distance value of abscissa axis, S = Distance value of ordinate axis)

It is important to mention that for unimodal data the mean can be used, but for multimodal data the ideal is to use the mode as the descriptive statistics. The equation for the mode (Eq. 3) is:

$$Mode = I + \frac{(f_o - f_{-1}) * h}{2f_o - (f_{-1}) - (f_{+1})} \quad (\text{Eq. 3})$$

where: I = lower limit of the modal class, f_0 = frequency of the modal class, f_{-1} = frequency of the preceding class, f_{+1} = frequency of the following class, and h = length of the class-interval.

TABLE I
Synthesis of the structural model proposed by Roldan (2007) related to the emplacement of the Lages Dome.

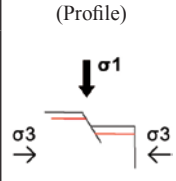
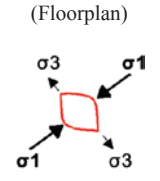
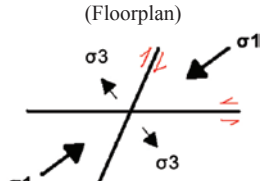
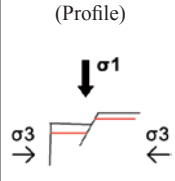
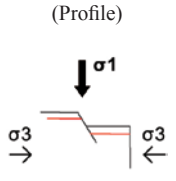
| AGE | Cretaceous (After the Serra Geral magmatic event) | Eo-Cretaceous (Dome emplacement) | Paleocene-Eocene (T) (After dome emplacement) | Eocene-Oligocene (T) | Miocene (T) | Pliocene (T) - Q |
|-----------------|--|--|--|----------------------|--|--|
| TECTONIC REGIME | Extensional | Compressive | Transcurrent | Tectonic Stability | Extensional | Extensional |
| σ_1 | Vertical | Horizontal NE-SW | Horizontal NE-SW | | Vertical | Vertical |
| FEATURE | Normal Faults | Major axis of the dome and emplacement of NE-SW dykes | Dextral strike-slip faults NNE-SSW/ NE-SW and sinistral strike-slip faults E-W | Erosion | Rio Canoas Lineament NW-SE | Normal faults NE-SW and strike-slip reactivation |
| | (Profile)  | (Floorplan)  | (Floorplan)  | | (Profile)  | (Profile)  |

TABLE II
 Value used to subtract the atmospheric influence in the LANDSAT ETM 7⁺ scenes, based on the “Simple Dark Pixel Subtraction” method (Chavez Jr 1975).

| SCENE/BAND | 221_079 | 220_079 |
|------------|---------|---------|
| BAND | 67 | 57 |
| BAND | 51 | 39 |
| BAND | 45 | 30 |
| BAND | 19 | 10 |
| BAND | 15 | 10 |
| BAND | 12 | 9 |

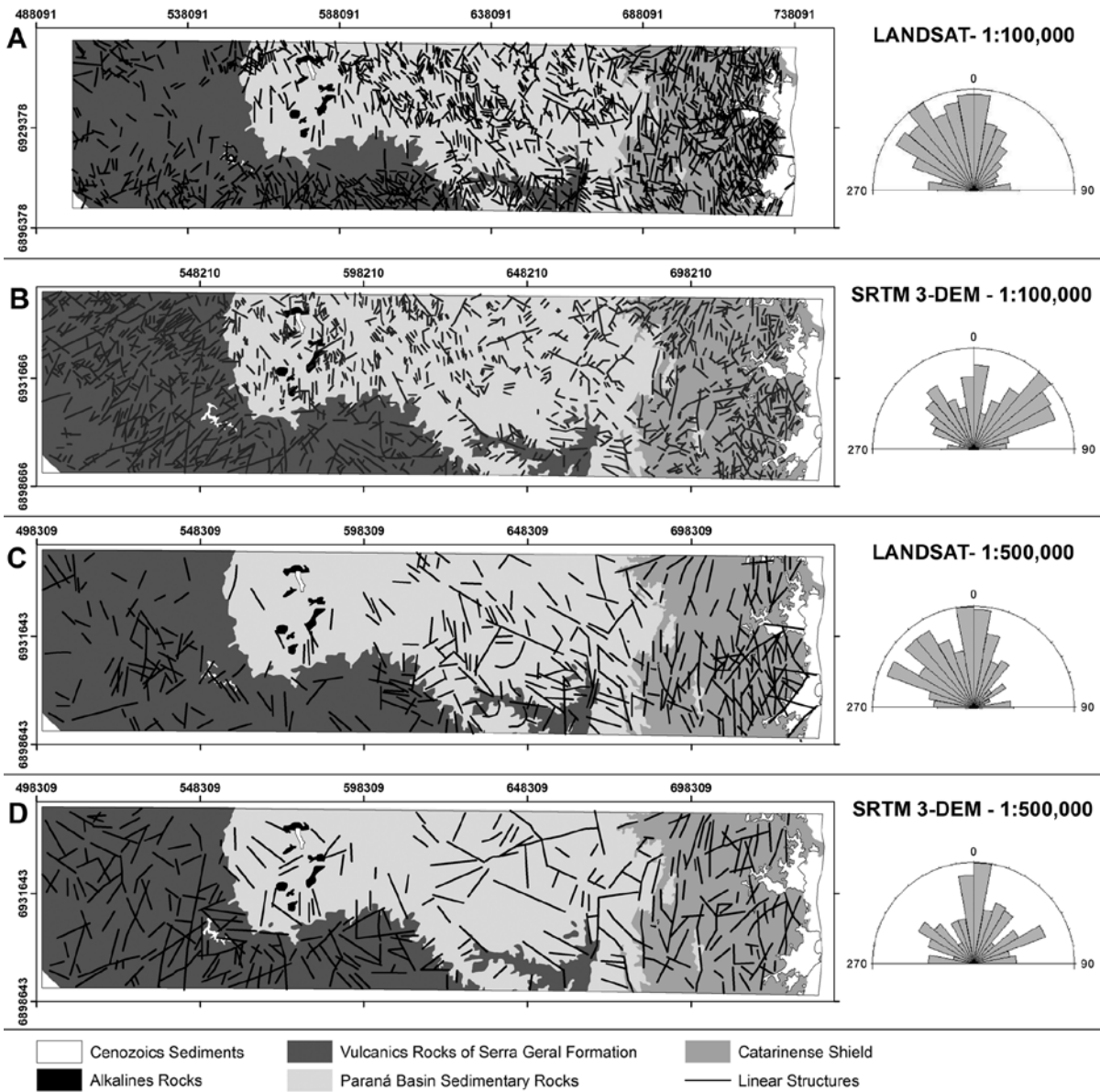


Figure 2 - Products obtained by visual interpretation: (A) LANDSAT at 1:100,000 scale; (B) SRTM at 1:100,000 scale; (C) LANDSAT at 1:500,000 scale and (D) SRTM at 1:500,000 scale and their respective rose diagram for total area.

TABLE III
Intervals of bi-directional data.

| Azimuth ϕ | Direction |
|----------------|-----------|
| 0°-30° | ENE/WSW |
| 31°-60° | NE/SW |
| 61°-90° | NNE/SSW |
| 91°-120° | NNW/SSE |
| 121°-150° | NW/SE |
| 151°-180° | WNW/ESE |

The circular variance (S_0^2) is used to demonstrate how the data are scattered around the mean and to compare the groups: the lower is its value, the smaller is the uncertainty. The variance is calculated based on the R value (Eq. 4) and divided by two since the data are bidirectional.

$$S_0^2 = (1-R)/2 \quad (\text{Eq. 4})$$

The circular standard deviation (s_0) (Eq. 5) is simply the square root of the variance and it is given in degrees.

$$s_0 = (2*S_0^2)^{1/2} \quad (\text{Eq. 5})$$

The cumulative frequency is used to compare the scales of each one of the images, in order to check whether the data represent the same population and if they can be used in multiscale studies.

RESULTS

The results are presented in Table IV, which shows that the lineaments extracted from the SRTM images are usually multimodal, except for the data related to Mesozoic rocks (1:100,000 scale). However, the 1:500,000 scale LANDSAT images are unimodal, except for the Proterozoic domain. The 1:100,000 scale LANDSAT images are multimodal, except for the Paleozoic rocks.

Comparing both from 1:500,000 LANDSAT and SRTM data scale, the general pattern presents different values for the mean, but the values for mode are closer, except for the Mesozoic data, whose mode values are N70W for LANDSAT and N25E for SRTM.

Examining modes obtained from both 1:100,000 scale LANDSAT and SRTM image we realize the values are completely different, except for the Paleozoic domain, in which main modes are similar.

Analyzing the circular standard deviations for all the data we conclude that lineaments extracted from the SRTM images vary more than those corresponding to LANDSAT images, although it does not happen with SRTM data for the Mesozoic domain (1:100,000 scale).

Considering each mode and circular standard deviation, Figure 3 shows a linear representation of the general lineaments extracted from SRTM and LANDSAT images at both scales. For the 1:500,000 scale the range of mode and circular standard deviation values for SRTM contains the range corresponding to LANDSAT. On the other hand, the same behavior does not happen for the 1:100,000 scale.

Figure 4A synthesizes the comparison between the 1:500,000 scale images by geological domain. For the Proterozoic and Paleozoic domains the range of SRTM data includes those of the LANDSAT images; although the variation of SRTM data is greater, mainly for the Paleozoic domain. However, for Mesozoic rocks the data are totally different.

The comparison of data corresponding to the 1:100,000 scale is shown in Figure 4B. There are no similarities, except for the Paleozoic data. Data obtained from SRTM images are generally dispersed.

The cumulative frequency used to compare the scales (Fig. 5) shows a high similarity between the products obtained for each type of image at both scales, indicating that they can be used in multiscale studies.

DISCUSSION

The comparison between LANDSAT and SRTM data shows that the lineaments extracted from the SRTM shaded relief images display a wide range of directions. This is expected because the final results for the SRTM images were obtained by the interpretation of four different shadow relief images obtained for

TABLE IV
Synthesis of the descriptive statistics after lineament extraction from LANDSAT and SRTM images at 1:500,000 and 1:100.000 scales. Patterns classified in general, Proterozoic, Paleozoic and Mesozoic domains. Highlighted cells refer to similar values.

| SRTM | 500_ general | 500_ Proteroz. | 500_ Paleoz. | 500_ Mesoz. | 100_ general | 100_ Proteroz. | 100_ Paleoz. | 100_ Mesoz. |
|-----------------------------|-----------------|-------------------|-----------------|----------------|-----------------|-------------------|-----------------|----------------|
| Angular Mean | 11 (N11E) | 8 (N8E) | 129 (N51W) | 20 (N20E) | 22 (N22E) | 22 (N22E) | 169 (N11W) | 52 (N52E) |
| Mode | N10E, N10W | N10E, N10W | N50W, N70E | N25E, N65E | N50E, N40W | N45E, N40W | N40W, NS±10 | N50E |
| Length | 0.131 | 0.329 | 0.014 | 0.076 | 0.151 | 0.226 | 0.225 | 0.263 |
| Circular Variance | 0.434 | 0.335 | 0.493 | 0.462 | 0.424 | 0.387 | 0.388 | 0.369 |
| Circular Standard Deviation | 57.712° | 42.708° | 83.806° | 64.963° | 55.7° | 49.374° | 49.518° | 46.829° |
| N | 312 | 87 | 82 | 150 | 1441 | 412 | 548 | 524 |
| LANDSAT | 500_ general | 500_ Proteroz. | 500_ Paleoz. | 500_ Mesoz. | 100_ general | 100_ Proteroz. | 100_ Paleoz. | 100_ Mesoz. |
| Angular Mean | 157 (N23W) | 174 (N6W) | 144 (N36W) | 144 (N36W) | 159 (N21W) | 168 (N12W) | 153 (N27W) | 155 (N25W) |
| Mode | N10E, N10W | N10E, N10W | N60W | N70W | N40W, NS (±10) | N10E, N10W | N40W | N60W, N10E |
| Length | 0.274 | 0.458 | 0.338 | 0.172 | 0.292 | 0.353 | 0.346 | 0.181 |
| Circular Variance | 0.363 | 0.271 | 0.331 | 0.414 | 0.354 | 0.323 | 0.327 | 0.41 |
| Circular Standard Deviation | 46.103° | 35.794° | 42.175° | 53.752° | 44.886° | 41.336° | 41.711° | 52.977° |
| N | 366 | 122 | 154 | 142 | 1573 | 538 | 655 | 478 |

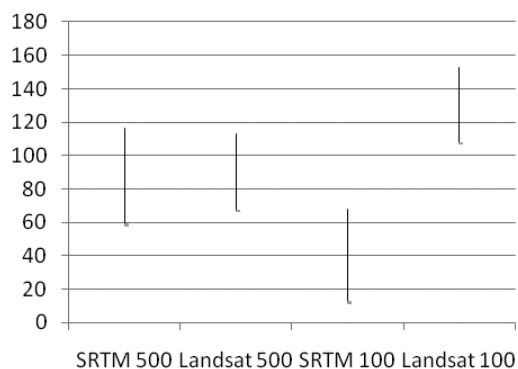


Figure 3 - General representation of lineaments extracted from SRTM and LANDSAT at both scales, based on the mode and circular standard deviation. The value 90 represents NS direction, value from 91 to 180 represents NW/SE directions and value 0 to 89 represents NE/SW directions.

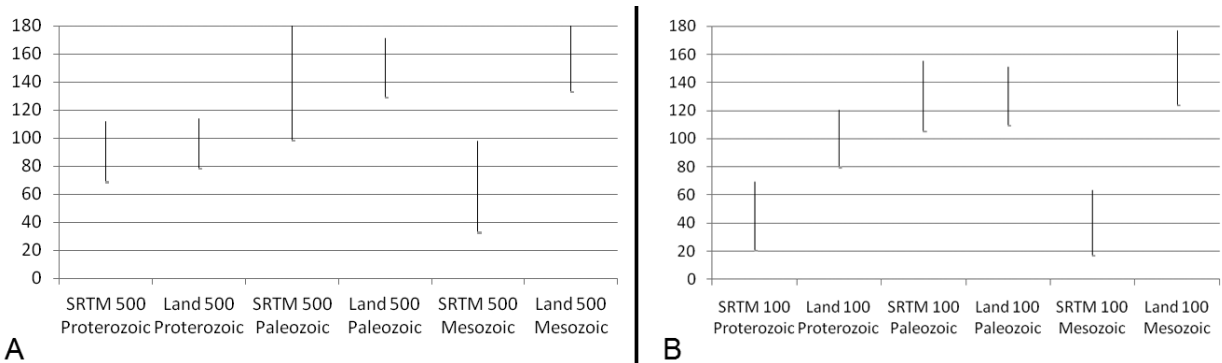


Figure 4 - Linear representation of the structures extracted from SRTM and LANDSAT at a 1:500,000 scale (A) and for 1:100,000 scale (B) for each geological domain, based on the mode and circular standard deviation. Value in ordinate axis represents azimuth.

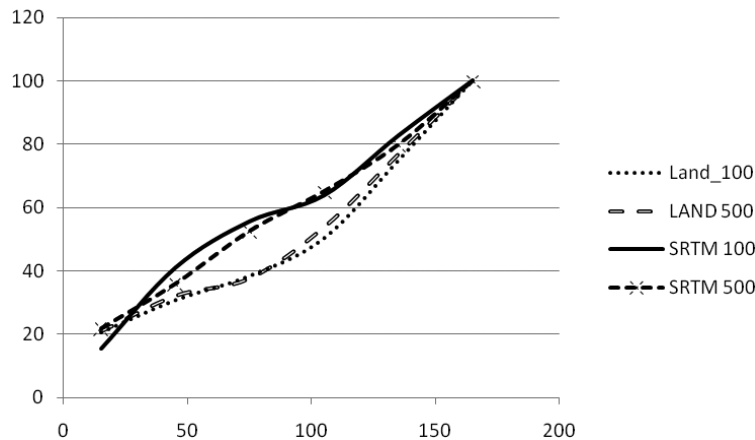


Figure 5 - Accumulated frequency used to compare the scales of the images.

azimuths 0°, 45°, 90° and 315°, whereas the Landsat data were extracted from two images corresponding to their sun azimuths (220_079 = 62.74 and 221_079 = 77.3) which value mean is nearly 70°.

The interpretation of such LANDSAT image depends on the solar azimuth, time and date of the passage of the satellite over the studied area, enhancing structures perpendicular to sunlight. In this case the solar azimuth is close to 48°, implying that lineaments parallel to this angle are concealed and that the structures perpendicular to it are stressed out. The NW-trending lineaments are thus highlighted, whereas the NE-trending lineaments are concealed, specially in the 1:100,000 scale images. The same discussion was made by Riccomini and Crósta

(1988) about Landsat images, that it is dependable of the season. Smith and Wise (2007) pointed that above 20° of solar elevation there is a gradual decrease in the relief effect for the Landsat images.

The similar pattern obtained for LANDSAT images at both scales suggests that the visual observation of lineaments does not depend on the scale, indicating that the LANDSAT images highlight the major features as continuous even at larger scales. This is indicated by the cumulative frequency curves (Fig. 5), that show the best overlap of the two LANDSAT curves, when compared to the SRTM curves. Therefore the LANDSAT images are more appropriate for multiscale studies in the studied area than the SRTM images.

For both 1:100,000 scale LANDSAT and SRTM data, different values were obtained for the geological domains, except for the Paleozoic rocks. One explanation for this difference is related to local tectonic stresses that are not evidenced by the LANDSAT image due to the single azimuth, especially the NE structures. These could be extracted from SRTM shadow relief images corresponding to different azimuths.

The Paleozoic domain is composed of sedimentary rocks, differently from the other domains that are constituted by igneous and metamorphic rocks. The same patterns resulted for each type of image at both scales, suggesting that rheology influences the pattern of the data extracted. For igneous and metamorphic rocks differences are observed and the main directions are dependent on the kind of image used. Conversely, there is no difference in the use of LANDSAT or SRTM images to extract lineaments affecting sedimentary rocks.

Among the geological domains of the studied area, the Mesozoic is more dependent on the type of used image. SRTM images yield the NE direction as the main mode, whereas the LANDSAT images highlighted NW-trending lineations, due to the influence of the solar azimuth.

The circular standard deviation close to 84° for SRTM (1:500,000) data corresponding to the Paleozoic sedimentary rocks may be associated with the Lages Dome. Table I presents a synthesis of the model proposed by Roldan (2007) that shows variations in lineament directions. While in the Miocene the main direction was NW-SE, in the Pliocene it changes to NE-SW. On the other hand, Landsat images could not register the NE directions as well as NW directions.

CONCLUSIONS

The $NS\pm 10$ general modal direction obtained from the 1:500,000 scale LANDSAT and SRTM images can represent the same population. For the 1:100,000 scale, the results are different and

opposite, indicating that for large scales they represent different populations. This can be caused by the four images derived from SRTM using different azimuths, contrarily to the single solar azimuth LANDSAT image.

The scales of each kind of remote sensing image were compared using the main mode and the circular variation. High similarity between each image product at both scales was observed, representing the same population and indicating that they can be used in multiscale studies.

For the Catarinense Shield the main direction is $NS\pm 10$ for LANDSAT (1:100,000 and 1:500,000) and for SRTM (1:500,000). The NE direction is shown by the SRTM images (1:100,000) but is not evident in the Landsat images, due to the 48° solar azimuth.

The Paraná Basin sedimentary rocks have similar mode values for both image types and scales, while the Mesozoic data are the most contrasting. Whereas SRTM stresses out NE directions, LANDSAT stresses out NW directions but not NE lineaments, due to the 70° mean solar azimuth, that enhance NW structures.

As a general conclusion both images can be used in lineament extraction at smaller scales (1:500,000), since the same population and the extensive linear structures are represented. However, for larger scales (1:100,000), the use of SRTM images is recommended because shadow relief images can be produced for different azimuths, and lineaments of different directions are thus highlighted.

ACKNOWLEDGMENTS

The authors wish to thank the Brazilian Geological Survey, Companhia de Pesquisa de Recursos Minerais (CPRM); the Post-Graduation Program in Minerals Resources and Hydrogeology of the Geosciences Institute of Universidade de São Paulo; the Universidade Federal Rural do Rio de Janeiro and the Faults and Fluid Flow Project (UFPR/PETROBRAS) for financial support. The

author thanks also the two anonymous reviewers for constructive criticisms of the manuscript and Kathleen Brookfield for the English revision.

RESUMO

Este artigo apresenta a comparação, através da estatística descritiva, de lineamentos de estruturas rúpteis obtidas manualmente sobre imagens Landsat e relevo sombreado do SRTM 3 MDE nas escalas 1:100.000 e 1:500.000. A área selecionada localiza-se no sul do Brasil e engloba rochas do pré-Cambriano e unidades estratigráficas da Bacia do Paraná. A aplicação desta metodologia demonstra que a interpretação visual depende do tipo de imagem do sensor remoto. O resultado da estatística descritiva obtido para os lineamentos extraídos das imagens não apresenta o mesmo padrão em função da escala adotada. A principal direção encontrada nas rochas do Proterozoico em ambas as imagens, na escala 1:500.000, é próxima de NS±10, enquanto que na escala 1:100.000 a direção N45E foi obtida nas imagens de relevo sombreado do SRTM 3 MDE e a direção N10W nas imagens Landsat. Rochas sedimentares Paleozóicas mostraram os melhores resultados para ambas as imagens e escalas (N50W). Por outro lado as rochas ígneas Mesozóicas mostraram as maiores diferenças, realçando as estruturas NE nas imagens SRTM 3 MDE e as estruturas NW nas imagens Landsat. A frequência acumulada demonstrou alta similaridade entre os produtos de cada tipo de imagem, independente da escala, indicando que podem ser utilizadas em estudos multiescala. Entretanto as maiores diferenças foram encontradas quando foram comparados os dados obtidos pelas imagens sombreadas do SRTM 3 MDE e imagens Landsat na escala 1:100.000.

Palavras-chave: imagens Landsat, sensoriamento remoto, SRTM, Santa Catarina, estatística, lineamentos estruturais.

REFERENCES

- ALMEIDA FFM. 1967. Origem e evolução da plataforma brasileira. Rio de Janeiro, DNPM/DGM, Boletim 241, 36 p.
- ALMEIDA FFM. 1969. Diferenciação tectônica da Plataforma Brasileira. Congresso Brasileiro de Geologia, 23, 1969, Salvador. Anais. Salvador: SBG, p. 29-46.
- ALMEIDA FFM. 1986. Distribuição regional e relações tectônicas do magmatismo pós-Paleozoico no Brasil. *Rev Bras de Geoc* 16(4): 325-349.
- ALMEIDA-FILHO R AND MIRANDA FP. 2007. Mega capture of the Rio Negro and formation of the Anavilhanas Archipelago, Central Amazônia, Brazil: Evidences in an SRTM digital elevation model. *Rem Sens Environ* 110: 387-392.
- BITENCOURT MF, BONGIOLO EM, PHILIPP RP, MORALES LFG, RUBERT RR, MELO CL AND LUFT Jr JL. 2008. Estratigrafia do Batólito Florianópolis, Cinturão Dom Feliciano, na Região de Garopaba-Paulo Lopes, SC. *Rev Pesq em Geoc (UFRGS)* 35: 109-136.
- CARPER JW, LILLESAND MT AND KIEFER WR. 1990. The Use of Intensity Hue-Saturation Transformations for Merging SPOT Panchromatic and Multispectral Image Data. *Photogram Eng Rem Sens* 56(4): 459-467.
- CHAVEZ JR PS. 1975. Atmospheric, solar and MTF corrections for ERTS digital imagery. Proceedings of the American Society of Photogrammetry, Fall Technical Meeting, Phoenix, AZ, 69 p.
- CREPANI E AND MEDEIROS JS. 1994. Imagens fotográficas derivadas de MNT do Projeto SRTM para fotointerpretação na Geologia, Geomorfologia e Pedologia./E. Crepani; J. S. de Medeiros. São José dos Campos: INPE.
- DEMIRKESEN AC. 2009. Quantifying geological structures of the Nigde province in central Anatolia, Turkey using SRTM DEM data. *Environ Geol* 56: 865-875.
- FARR TG ET AL. 2007. The Shuttle Radar Topography Mission. *Rev Geophys* 45(2): 21-35.
- GROHMANN CH, RICCOMINI C AND ALVES FM. 2007. SRTM-based morphotectonic analysis of the Poço de Caldas Alkaline Massif, Southeastern Brazil. *Comput Geosci* 33: 10-19, doi: 10.1016/j.cageo.2006.05.002.
- GUTH PL. 2006. Geomorphometry from SRTM: Comparison to NED. *Photogram Eng Rem Sens* 72: 269-278.
- HORN FILHO NO. 2003. Setorização da Província Costeira de Santa Catarina em base aos aspectos geológicos, geomorfológicos e geográficos. *Geosul, Florianópolis* 18(35): 71-98.
- HORN FILHO NO AND DIEHL FL. 1994. Geologia da Planície Costeira de Santa Catarina. *Alcance. UNIVALI* 1(1): 95-102.
- HORN FILHO NO AND DIEHL FL. 2001. Geologia da Planície Costeira de Santa Catarina. Congresso do Quaternário de países de línguas ibéricas. Lisboa, 2001. *Actas Lisboa: GTPEQ, AEQUA, SGP*, p. 203-206.
- JORDAN G, MEIJNINGER BML, HINSBERGEN DJJV, MEULENKAMP JE AND DIJK PMV. 2005. Extraction of morphotectonic features from DEMs: Development and applications for study areas in Hungary and NW Greece. *Int J Appl Earth Observ Geoinf* 7(3): 163-182.
- KOIKE K, NAGAMO S AND OHMI M. 1995. Lineament analysis of satellite images using a Segment Tracing Algorithm (STA). *Comp and Geosc* 21(9): 1091-1104.
- MARDIA KV. 1972. *Statistics of Directional Data*. Academic Press, London, New York, 357 p.

- MASOUD A AND KOIKE K. 2006. Tectonic architecture through Landsat-7ETM⁺/SRTM DEM - derived lineaments and relationship to the hydrogeologic setting in Siwa region, NW Egypt. *J Afr Earth Sci* 45: 467-477.
- MORGAN WJ. 1981. Hotspot tracks and the opening of the Atlantic and Indian oceans. In: *The Sea*, edited by C. Emiliani, J Wiley & Sons, New York, p. 443-487.
- O'CONNOR JM AND DUNCAN RA. 1990. Evolution of the Walvis Ridge - Rio Grande Rise hot spot system: Implications for African and South American plate motions over plumes. *J Geophys Res* 95(B11): 17475-17502.
- O'LEARY DW, FRIEDMAN JD AND POHN HA. 1976. Lineament, linear, lineation: some proposed new standards for old terms. *Bull Geol Soc Am* 87: 1463-1469.
- PASSARELLI CR. 1996. Análise estrutural e caracterização do magmatismo da zona de cisalhamento Major Gercino, SC. Dissertação de Mestrado, Instituto de Geociências, Universidade de São Paulo, São Paulo, 178 p. (Unpublished).
- PICCIRILLO EM, BELLIENI G, CAVAZZINI H, COMIN-CHIARAMONTI P, PETRINI R, MELFI AJ, PINESE JPP, ZANTADESCHI P AND DE MIN A. 1990. Lower Cretaceous tholeiitic dyke swarms in the Ponta Grossa Arch (South East Brazil): petrology, Sr-Nd isotopes, and genetic relationships from Paraná flood volcanic. *Chem Geol* 89: 19-48.
- RAMLI MF, YUSOF N, YUSOFF MK, JUAHIR H AND SHAFRI HZM. 2010. Lineament Mapping and its application in landslide hazard assessment: a review. *Bull Eng Geol Environ* 69: 215-233.
- RENNE PR, ERNESTO M, PACCA IG, COE RS, GLEN JM, PRÉVOT M AND PERRIN M. 1992. The age of Paraná flood volcanism, rifting of Gondwanaland, and the Jurassic-Cretaceous Boundary. *Science* 258: 975-978.
- RICCOMINI C AND CRÓSTA AP. 1988. Análise preliminar de lineamentos em produtos de sensores remotos aplicada à prospecção mineral na área dos granitóides Mandira, SP. *Boletim IG-USP. Série Científica*, São Paulo 19: 23-37.
- RODRIGUES TG, PARADELLA WR AND OLIVEIRA CG. 2011. Evaluation of the altimetry from SRTM-3 and planimetry from high-resolution PALSAR FBD data for semi-detailed topographic mapping in the Amazon Region. *An Acad Bras Cienc* 83: 953-966.
- ROLDAN LF. 2007. Tectônica Rúptil Meso-Cenozóica na região do Domo de Lages, SC. Dissertação (Mestrado) – Instituto de Geociências, Universidade de São Paulo, São Paulo, 121 p. (Unpublished).
- ROSSETTI D AND VALERIANO MM. 2007. Evolution of the lowest amazon basin modeled from the integration of geological and SRTM topographic data. *Catena* 70: 253-265.
- SILVA CL, MORALES N, CRÓSTA AP, COSTA SS AND JIMÉNES-RUEDA JR. 2007. Analysis of tectonic-controlled fluvial morphology and sedimentary processes of the western Amazon Basin: an approach using satellite images and digital elevation model. *An Acad Bras Cienc* 79: 693-711.
- SMITH MJ AND WISE SM. 2007. Problems of bias in mapping linear landforms from satellite imagery. *Int J Appl Earth Observ Geoinf* 9: 65-78.
- STRIEDER AJ AND AMARO VE. 1997. Structural patterns removed from remotely sensed lineaments. *Rev Esc Eng* 25(4): 109-117.
- TURNER RE, MALILA WA AND NALEPKA RF. 1971. Importance of atmospheric scattering in remote sensing or everything you've always wanted to know about atmospheric scattering but were afraid to ask. *Proc of the Seventh Int. Symp. on Rem Sens Environ* 3: 1651-1697.
- VALERIANO MM, KUPLICH TM, STORINO M, AMARAL BD, MENDES JR JN AND LIMA DJ. 2006. Modeling small watersheds in Brazilian Amazonia with shuttle radar topographic mission-90m data. *Comp and Geosc* 32: 1169-1181.
- ZALÁN PV, WOLFF S AND CONCEIÇÃO JC. 1987. Tectônica e sedimentação da Bacia Sedimentar do Paraná. In: *Simpósio Sul-brasileiro de Geologia 3º*, 1987, Curitiba. *Atas* 1: 441-474.
- ZALÁN PV, WOLFF S, CONCEIÇÃO JC, ASTOLFI MAM, VIEIRA IS, APPI CT, ZANOTTO AO AND MARQUES A. 1991. Tectonics and sedimentation of the Paraná Basin. *Seventh International Gondwana Symposium, Gondwana Seven, Proceeding*. São Paulo, Brazil, p. 83-117.